Article

A Highly π-Stacked Organic Semiconductor for Field-Effect Transistors Based on Linearly Condensed Pentathienoacene

Kai Xiao, Yunqi Liu, Ting Qi, Wei Zhang, Fang Wang, Jianhua Gao, Wenfeng Qiu, Yongqiang Ma, Guanglei Cui, Shiyan Chen, Xiaowei Zhan, Gui Yu, Jingui Qin, Wenping Hu, and Daoben Zhu

J. Am. Chem. Soc., **2005**, 127 (38), 13281-13286• DOI: 10.1021/ja052816b • Publication Date (Web): 25 August 2005

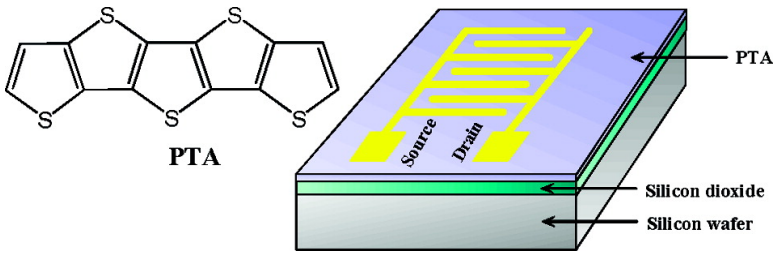

More About This Article

Additional resources and features associated with this article are available within the HTML version:

- Supporting Information
- Links to the 49 articles that cite this article, as of the time of this article download
- Access to high resolution figures
- Links to articles and content related to this article
- Copyright permission to reproduce figures and/or text from this article

View the Full Text HTML

J|A|C|S
ARTICLES
Published on Web 08/25/2005

A Highly π-Stacked Organic Semiconductor for Field-Effect Transistors Based on Linearly Condensed Pentathienoacene

Kai Xiao,[†] Yunqi Liu,*[,†] Ting Qi,[†] Wei Zhang,[‡] Fang Wang,[‡] Jianhua Gao,[†] Wenfeng Qiu,[†] Yongqiang Ma,[†] Guanglei Cui,[†] Shiyan Chen,[†] Xiaowei Zhan,[†] Gui Yu,[†] Jingui Qin,*[,‡] Wenping Hu,[†] and Daoben Zhu*[,†]

Contribution from the Key Laboratory of Organic Solids, Institute of Chemistry, Chinese Academy of Sciences, Beijing 100080, P.R. China, and Department of Chemistry, Wuhan University, Wuhan 430072, P.R. China

Received April 29, 2005; E-mail: liuyq@mail.iccas.ac.cn

Abstract: We present the synthesis and characterization of a fused-ring compound, dithieno[2,3-*d*:2′,3′-*d*′]thieno[3,2-*b*:4,5-*b*′]dithiophene (pentathienoacene, PTA). In contrast to pentacene, PTA has a larger band gap than most semiconductors used in organic field-effect transistors (OFETs) and therefore is expected to be stable in air. The large π-conjugated and planar molecular structure of PTA would also form higher molecular orders that are conductive for carrier transport. X-ray diffraction and atomic force microscopy experiments on its films show that the molecules stack in layers with their long axis upright from the surface. X-ray photoelectron spectroscopy suggests that there are no chemical bonds at the PTA/Au interface. OFETs based on the PTA have been constructed, and their performances as p-type semiconductors are also presented. A high mobility of 0.045 cm^2/V s and an on/off ratio of 10^3 for a PTA OFET have been achieved, demonstrating the potential of PTA for application in future organic electronics.

Introduction

Organic semiconductors employed as active layers in field-effect transistors (FETs) are of great current interest because such FETs can potentially be fabricated at low cost, over large areas, and on flexible substrates.[1] Such facile fabrication approaches offer a significant advantage over silicon technology in numerous applications. Much progress on organic FETs has been made in various organic-based electronic circuits, such as displays,[2] sensor,[3] inverts, and logic elements.[4] Of all the OFET materials reported so far, the highest mobility has been recorded for pentacene (0.3−0.7 cm^2/V s on SiO_2/Si and 1.5 cm^2/V s on chemically modified SiO_2/Si).[5] The highest occupied molecular orbital (HOMO) energy level in linearly condensed [*n*]acenes significantly increases with increasing *n*, which facilitates the formation of radical cations (holes) at the interface between a dielectric and a semiconducting layer. Furthermore, the extended π system of a higher acene enhances the intermolecular overlap of $\pi-\pi$ systems in the solid state and leads to high mobility.[6] However, pentacene suffers from the disadvantages of oxidative instability, extreme insolubility, and, for display applications, a strong absorbance throughout the visible spectrum.[7] Where photoinduced decomposition reactions could occur, this absorbance would make pentacene sensitive to most visible light. Compared to pentacene, an important small molecule semiconductor that is rigidly planar, thiophene-based materials exhibit a variety of intra- and intermolecular interactions—van der Waals interactions, weak hydrogen bondings, $\pi-\pi$ stacking, sulfur−sulfur interactions—originating from the high polarizability of sulfur electrons in the thiophene rings.[8] Therefore, thiophene-based materials are a promising class of organic materials for their use in organic thin film transistors.[9] Oligothiophenes have been widely used as organic devices materials, but they can easily twist from planarity, thus disrupting conjugation and potentially affecting band gap in the solid state. An intriguing approach for the design of conjugated small molecules is to combine the stability of the thiophene ring with the planarity of linear acenes to produce fused-ring thienoacenes. However, fused-ring thiophenes are more difficult to synthesize than oligothiophenes. As an example, a conjugated oligomer contain-

[†] Chinese Academy of Sciences.
[‡] Wuhan University.

(1) (a) Dimitrakopoulos, C. D.; Malenfant, P. R. L. *Adv. Mater.* **2002**, *14*, 99−117. (b) Horowitz, G. *Adv. Mater.* **1998**, *10*, 365−377.
(2) (a) Mitschke, U.; Bäuerle, P. *J. Mater. Chem.* **2000**, *10*, 1471−1507. (b) Wisnieff, R. *Nature* **1998**, *394*, 225−227. (c) Comiskey, B.; Albert, J. D.; Yoshizawa, H.; Jacobsen, J. *Nature* **1998**, *394*, 253−255.
(3) (a) Crone, B.; Dodabalapur, A.; Lin, Y.-Y.; Filas, R. W.; Bao, Z.; LaDuca, A.; Sarpeshkar, R.; Katz, H. E.; Li, W. *Nature* **2000**, *403*, 521−523. (b) Lin, Y.-Y.; Dodabalapur, A.; Sarpeshkar, R.; Bao, Z.; Li, W.; Baldwin, K.; Raju, V. R.; Katz, H. E. *Appl. Phys. Lett.* **1999**, *74*, 2714−2716.
(4) (a) Bartic, C.; Palan, B.; Campitelli, A.; Borghs, G. *Sens. Actuators, B* **2002**, *83*, 115−122. (b) Crone, B.; Dodabalapur, A.; Gelperin, A.; Torsi, L.; Katz, H. E.; Lovinger, A. J.; Bao, Z. *Appl. Phys. Lett.* **2001**, *78*, 2229−2231.
(5) (a) Gundlach, D. J.; Lin, Y.-Y.; Jackson, T. N.; Nelson, S. F.; Schlom, D. G. *IEEE Electron Device Lett.* **1997**, *18*, 87−89. (b) Lin, Y.-Y.; Gundlach, D. J.; Nelson, S. F.; Jackson, T. N. *IEEE Electron Device Lett.* **1997**, *18*, 606−608.
(6) Ito, K.; Suzuki, T.; Sakamoto, Y.; Kubota, D.; Inoue, Y.; Sato, F.; Tokito, S. *Angew. Chem. Int. Ed.* **2003**, *42*, 1159−1162.
(7) Yamada, M.; Ikemoto, I.; Kuroda, H. *Bull. Chem. Soc. Jpn.* **1988**, *61*, 1057−1062.
(8) (a) Marseglia, E. A.; Grepioni, F.; Tedesco, E.; Braga, D. *Mol. Cryst. Liq. Cryst.* **2000**, *348*, 137−151. (b) Barbarella, G.; Zambianchi, M.; Bongini, A.; Antolini, L. *Adv. Mater.* **1993**, *5*, 834−838.
(9) (a) Horowitz, G. *J. Mater. Chem.* **1999**, *9*, 2021−2026. (b) Katz, H. E.; Bao, Z. *J. Phys. Chem. B* **2000**, *104*, 671−678.

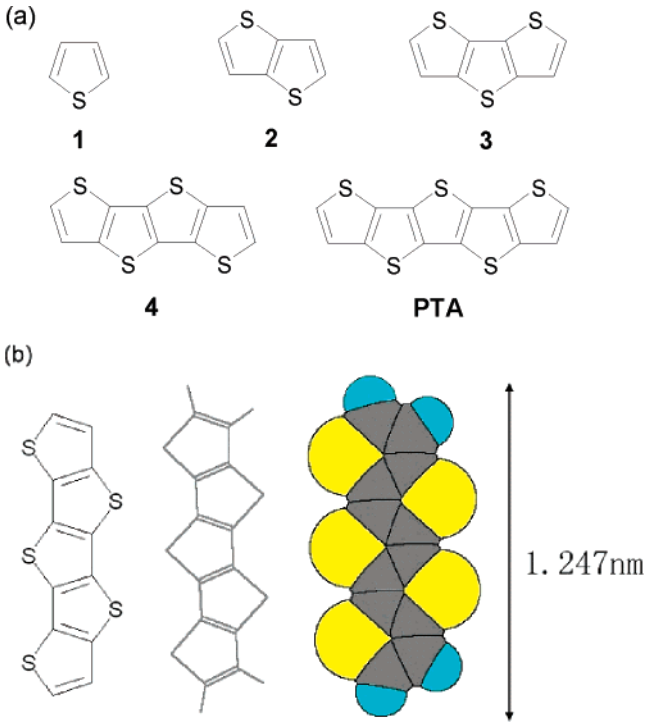

Figure 1. (a) Chemical structures of fused-ring oligothiophenes, thiophene (**1**), thieno[3,2-*b*]thiophene (**2**), dithieno[3,2-*b*:2′,3′-*d*]thiophene (**3**), thieno-[2″,3″:4′,5′:2′,3′-*d*:3,2-*b*:4,5-*b*]thiephene (**4**), and PTA. (b) The chemical structure and molecular model of PTA.

ing fused-ring thiophenes has been reported, e.g., 3,6-dimethylthieno[3,2-*b*]thiophene.[10] However, the steric repulsion between the β-methyl groups prevents coplanarity of adjacent thieno[3,2-*b*]thiophene units.[11] In addition, the *R*-linked dimer of dithieno[3,2-*b*:2,3-*d*]thiophene (**3**) and its alkylated derivatives have proven to be effective as the active layer in organic thin film transistors (TFTs).[12] Higher thienoacene with $n = 4$ has also been reported, and a crystal structure has been obtained that indicates the planarity of these fused-ring systems.[13] Pentathienoacene ($n = 5$, PTA, Figure 1) was attractive because it combined the molecular shape of pentacene, which leads to a favorable crystal packing geometry and orientation, with thiophene monomer, which would increase stability and nuclear aromaticity and also provide points of attachment for solubilizing substituents. These molecules bear essentially less hydrogen atoms in the molecular periphery and therefore are expected to interact efficiently through intermolecular S−S contacts. Therefore, the linearly condensed thiophenes would give the most extended π conjugation and the highest planarity. On the basis of the ring system, PTA would be expected to have a suitable HOMO energy and solid-state structure for use as a p-channel TFT semiconductor. Moreover, the susceptibility of the C−H bonds at the ends of PTA presents an avenue for end substitution, so that the solubility, morphology, and adhesion could be

Scheme 1. Synthetic Routes of PTA

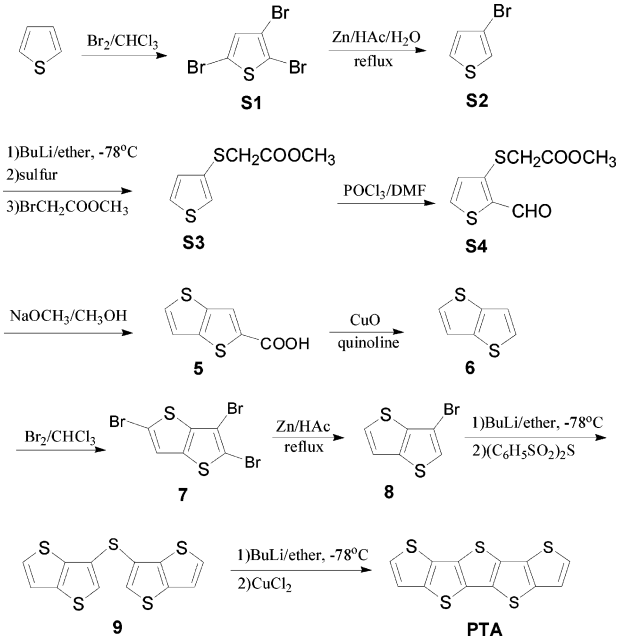

better defined. Such a PTA semiconductor has the general attributes of not absorbing in the visible region of the spectrum (larger band gaps) and possessing reasonable stability against oxidative doping by atmospheric oxygen. However, probably because of the lack of convenient synthetic routes, devices utilizing these fused-ring compounds have not been studied.

Here we present the synthesis and characterization of PTA. In contrast to pentacene, PTA has a larger band gap than most semiconductors used in OTFTs and is therefore expected to be stable in air. The large and planar molecular structure of PTA would also form higher molecular orders that are conductive to carrier transport. OTFTs based on the PTA have been constructed, and their performances as p-type semiconductors are also presented.

Results and Discussion

PTA has been synthesized as shown in Scheme 1. Compounds **S1**, **S2**, **S3**, **S4**, **5**, **6**, **7**, and **8** were synthesized according to the methods described in the literature (see Supporting Information). Treatment of **8** with *n*-butyllithium and bis(phenylsulfonyl) sulfide could generate sulfide **9** in 41% yield. The yield of the oxidative ring closure of **9** was moderate (15−25%), presumably due to the low solubility of **9**. Pure PTA was isolated by column chromatography on silica gel as a yellowish solid. The compound is lighter in color and more environmentally stable than pentacene. The PTA is slightly soluble in THF, but pentacene is only sparingly soluble in high boiling point aromatic solvents. After purified by sublimation, PTA is a slightly yellow crystalline solid. Its chemical structure was determined by EI-MS and elemental analysis.[14] The thermal property of PTA was evaluated by thermogravimetric analysis (TGA). The TGA scan is shown in Figure 2, and an onset temperature of 272.46 °C is observed, demonstrating a higher thermal stability.

The UV−vis absorption spectrum for PTA in chloroform solution shows absorption peaks at 305, 317, 339, 344, and 358

(10) Nakayama, J.; Dong, H. B.; Sawada, K.; Ishii, A.; Kumakura, S. *Tetrahedron* **1996**, *52*, 471−488.
(11) Sotgiu, G.; Zambianchi, M.; Barbarella, G.; Aruffo, F.; Cipriani, F.; Ventola, A. *J. Org. Chem.* **2003**, *68*, 1512−1520.
(12) (a) Li, X. C.; Sirringhaus, H.; Garnier, F.; Holmes, A. B.; Moratti, S. C.; Feeder, N.; Clegg, W.; Teat, S. J.; Friend, R. H. *J. Am. Chem. Soc.* **1998**, *120*, 2206−2207. (b) Morrison, J. J.; Murray, M. M.; Li, X. C.; Holmes, A. B.; Moratti, S. C.; Friend, R. H.; Sirringhaus, H. *Synth. Met.* **1999**, *102*, 987−988.
(13) (a) Mazaki, Y.; Kobayashi, K. *J. Chem. Soc. Perkin Trans. 2* **1992**, 761−764. (b) Sato, N.; Mazaki, Y.; Kobayashi, K.; Kobayashi, T. *J. Chem. Soc. Perkin Trans. 2* **1992**, 765−770.

(14) See Supporting Information for the experimental details.

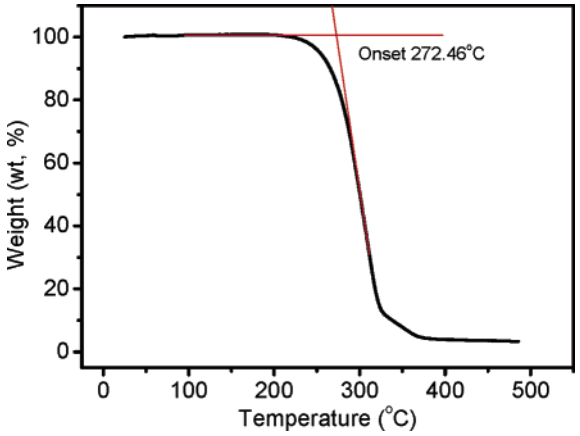

Figure 2. TGA measurements for PTA. The heating rate is 10 °C/min under N_2.

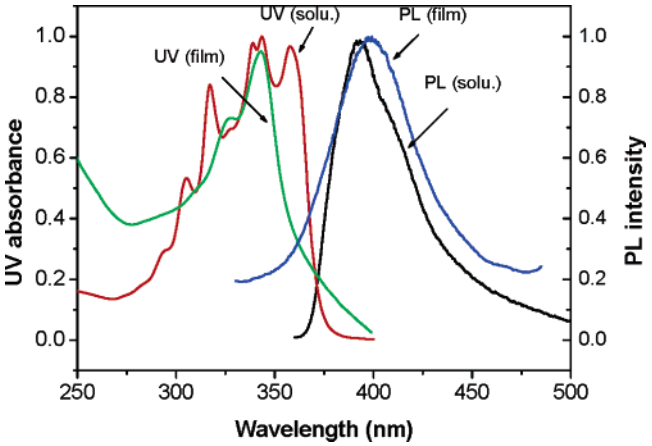

Figure 3. The absorption and emission spectra of PTA. UV−vis was measured in chloroform solution. The solution PL was excited at 344 nm and the solid-state PL at 260 nm.

nm (Figure 3). It is generally recognized that increasing the planarity of aromatic systems leads to more extensive conjugation and a corresponding decrease in the HOMO−lowest unoccupied molecular orbital (LUMO) gap. However, the increased sulfur substitution is widening it.[15] The LUMO of *R*-terethiophene has the appropriate symmetry for interacting with the sulfur atoms introduced at the positions in PTA; this effect is presumed to result from a destabilization of this orbital. The spectral absorption of vacuum-deposited thin films of PTA was slightly blue shifted, with absorption maxima at 326 and 342 nm, indicating that H-aggregates were formed. The solution photoluminescence (PL) was excited at 344 nm, and the solid-state PL was at 260 nm. PTA exhibits blue fluorescence in the solid state and a blue emission when irradiated in dilute solution with UV light. An HOMO−LUMO gap of 3.20 eV in dilute chloroform solution was estimated from the absorption edge. Cyclic voltammetry experiments were conducted using an Ag/AgCl reference and a glass carbon working electrode in 0.1 M Bu_4NPF_6/THF solution and showed two irreversible processes with an onset oxidation potential at 1.12 V and an onset reduction potential at −2.17 V, corresponding to an estimated HOMO level of −5.33 eV, a LUMO level of −2.04 eV, and a band gap (E_g) of 3.29 eV, respectively (see the Supporting Information). It is worth noting that the band gap (3.29 eV)

(15) Zhang, X.; Matzger, A. J. *J. Org. Chem.* **2003**, *68*, 9813−9815.

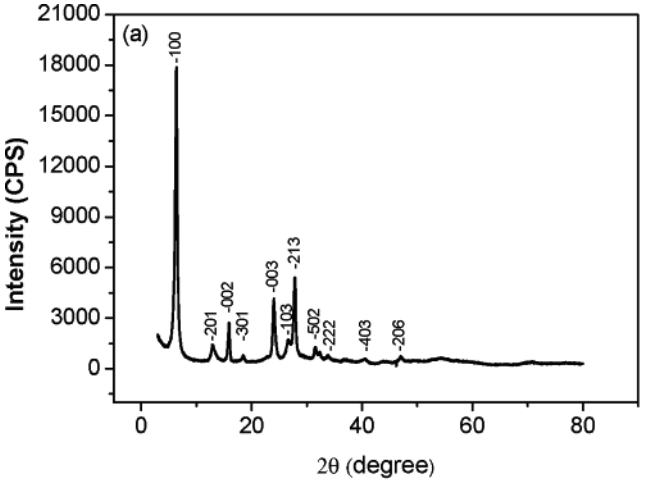

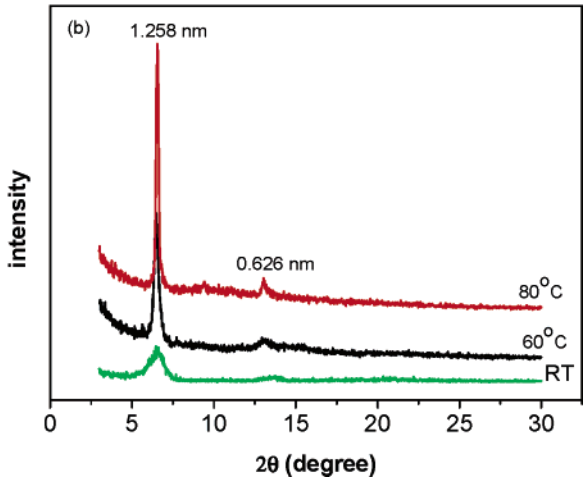

Figure 4. (a) X-ray diffraction patterns of a powder of sublimed PTA. (b) X-ray diffractograms of PTA films on SiO_2/Si fabricated at T_{sub} = room temperature, 60 and 80 °C.

obtained from the electrochemical measurement agrees well with the result (3.20 eV) determined by the absorption spectrum of the PTA. The value of the HOMO level is lower than those of most polythiophenes and pentacene, thus indicate higher oxidative stability. In pentacene, the band gap from the absorption edge is around 1.85 eV (670 nm).[16] Therefore, the band gap of PTA (3.29 eV) is significantly higher than that of pentacene, indicating a higher redox stability. The longest wavelength absorption for pentacene is shifted by ca. 80 nm on going from solution to thin film due to the association between the molecules in the solid state.[16] In contrast, the shift for PTA is only around 15 nm from solution to a film. This low amount of shifting for PTA upon film formation indicates the strong $\pi-\pi$ interactions of the molecules.

The powder X-ray diffraction pattern of PTA was recorded in transmission mode on a Siemens D5000 diffractometer at ambient temperature (Figure 4a). It has been reported that the crystalline phase of some materials can be obtained from the powder XRD files.[17] The powder diffraction pattern was indexed by the program Power-X[17] to give the following unit cell with

(16) (a) Boronat, M.; Viruela, R.; Ort, E. *Synth. Met.* **1995**, *71*, 2291−2295. (b) Kim, K.; Yoon, Y. K.; Mun, M.-O.; Park, S. P.; Kim, S. S.; Im, S.; Kim, J. H. *J. Supercond.* **2002**, *15*, 595−598. (c) Siebrand, W.; Zgierski, M. Z. *Springer Ser. Solid-State Sci.* **1983**, *49*, 136−144. (d) Yakeshi, T.; Goto, T.; Fujita, K.; Tsutsui, T. *Appl. Phys. Lett.* **2004**, *85*, 2098−2100.

monoclinic metric symmetry: $a = 14.521$ Å, $b = 6.144$ Å, $c = 11.628$ Å, $\alpha = 90°$, $\beta = 106.9648°$, $\gamma = 90°$. The crystal structure of PTA should be similar to the structure of **4**, in that each five-membered ring in the molecule is planar and the molecule as a whole is essentially planar.[13] Mazaki and Sato have investigated characteristic molecular aggregations in crystals of a series of linearly condensed thiophenes using photoelectron spectroscopy and determined the crystal and molecular structure of **4**.[13] The increase in molecular size of aromatic hydrocarbons with planar molecular structure can cause a decrease in the molecular packing density, due to an extension of the region for electron delocalization. But the polythiophene **4** and PTA have significantly larger polarization energy than **2** and **3**, which indicates that the balance between the molecular packing and the molecular polarizability is no longer held for **4** and PTA. Moreover, the crystal structure analysis has demonstrated an overly tightly packed arrangement of **4** with notably short intermolecular sulfur−sulfur contacts, whereas no such short contacts are found in the crystals of **3** and **2**. Therefore, an additive intermolecular interaction for PTA should be operating in the solid, which is explained by an additional sulfur atom with a further extended π system and from the overtight molecular packing density. Desiraju and Gavezzotti have explored a systematic analysis of the crystal structure of polynuclear aromatic hydrocarbons and have defined four basic packing types based on the shortest crystallographic axis (SA):[18] herringbone packing (SA > 5.4 Å), sandwich−herringbone packing, γ-type (4.6 > SA > 4.0 Å) and β-type (SA < 4.0 Å). These packing patterns are associated with the C:H stoichiometric ratios of the aromatic hydrocarbons. Thus, linearly condensed polynuclear aromatic hydrocarbons are more likely to use C−H interactions and to select herringbone packing, in which the mean plane of one molecule is steeply inclined to that of its nearest neighbors. Despite its geometrical similarity with hydrocarbon acenes, fused-ring thiophene does not pack in a herringbone motif, which is obviously attributable to the small number of hydrogen atoms in the molecular periphery. The C:S ratio in the molecular periphery is an important factor in engineering the short axis structure for planar sulfur heterocycles. Thus, the C:S ratio in a series of fused-ring thiophenes increases in the order PTA > **4** > **3** > **2**. It is likely that there is a threshold of C:S ratio that leads to short directional molecular contacts. The short molecular contacts together with the orbital interactions can serve in organizing the molecular aggregation into two-dimensional motifs. Therefore, compared to the structure of **4**, the crystal packing of PTA should also have two short intermolecular S−S contacts, which leads to side-by-side molecular arrangements with bay regions of a molecule gearing alternately into sulfur atoms of the adjacent molecules.

Figure 4b shows the XRD profile of a vacuum-evaporated thin film about 60 nm thick at different substrate temperatures (T_{sub}). X-ray diffraction profiles of PTA films indicate a primary diffraction peak at $2\theta = 6.51°$ (d-spacing 1.258 nm) with the second-order diffraction peaks at $2\theta = 13.04°$ (d-spacing 0.626 nm). The same angular position of the reflections indicates that both film and powders exhibit the same crystalline phase. The first of these corresponds exactly to the length of the PTA molecule, and the others are its second orders. In all films, the first-order reflection is very intense, and many films exhibit well-resolved higher order reflections as well, indicating well-ordered, layered microstructures. The same structure, high order, and lamellar shape were also found for the samples deposited at the higher temperatures. This type of orientation has been found particularly useful in achieving high mobilities since the $\pi-\pi$ stacking direction is in the plane of the current flowing direction.[19,20]

The crystalline structures in the vacuum-deposited thin films of PTA at different substrate temperatures can be directly examined by atomic force microscope. Figure 5 is the AFM images of PTA deposited on SiO_2 surface at three different substrate temperatures. Densely packed grains with average diameter of about 300−600 nm were observed in the thin film deposited at room substrate temperature, which indicated high crystallinity and three-dimensional order. The crystal grains grew in size with increasing substrate temperature. When substrate temperature is up to 80 °C, the crystal grain was relatively large and elongated in shape, with the average grain size being about 0.8×2 μm. The very sharp and narrow diffraction spots can be seen in the selected-area electron diffraction pattern, indicating the formation of single crystal domains, which is similar to single-crystal-type morphologies of pentacene film by direct evaporation (see the Supporting Information).[21]

For TFT application, the presence of a barrier at the interface of electrode and organic can modify the electron characteristics of the transistor. Therefore, it is very important to study the organic−inorganic interface. The electronic structure of the interface formation for PTA was investigated using X-ray photoelectron spectroscopy (XPS) (Figure 6). It shows the C 1s and S 2p binding energy (BE) as PTA is deposited onto a clean Au surface. Changes of the peak shape or the energetic position of the core level spectra are crucial for the analysis of interactions and the energy level alignment at interfaces. Starting at 2.0 nm of PTA deposition, the C 1s peak shifts to lower BE and saturates at −0.2 eV. This gradual shift can be attributed to changing polarization of the PTA layer as it becomes thicker atop the metal surface.[22] Its width is gradually reduced at higher coverage. The narrowing of the C 1s peak as more PTA is deposited onto the surface is expected, regardless of whether there is a chemical reaction due to the increasing uniformity of the environment of the individual PTA molecules as the PTA layer becomes thicker.[23] The sulfur atoms of the thiophene groups are also affected in the early stages of interface formation, as shown in Figure 6b. Starting at 2.0 nm of PTA deposition, the S 2p peak shifts to higher BE and saturates at 2.0 eV. The absence of special features at the earliest stages of deposition of PTA on Au in both the S 1s and the corresponding S 2p spectra indicate that no chemical reaction occurs at these interfaces independent of the orientation of the PTA molecules.[24]

(17) (a) Desiraju, G. R.; Gavezzotti, A. *J. Chem. Soc., Chem. Commun.* **1985**, *41*, 907−908. (b) Desiraju, G. R.; Gavezzotti, A. *Acta Crystallogr., Sect. B.* **1989**, *45*, 473−482.
(18) (a) Dong, C. *J. Appl. Cryst.* **1999**, *32*, 838−839. (b) Porzio, W.; Destri, S.; Mascherpa, M.; Bruckner, S. *Acta Polym.* **1993**, *44*, 266−272. (c) Melucci, M.; Gazzano, M.; Barbarella, G.; Cavallini, M.; Biscarini, F.; Maccagnani, P.; Ostoja, P. *J. Am. Chem. Soc.* **2003**, *125*, 10266−10274.
(19) Wu, Y.; Li, Y.; Gardner, S.; Ong, B. S. *J. Am. Chem. Soc.* **2005**, *127*, 614−618.
(20) Meng, H.; Bao, Z.; Lovinger, A. J.; Wang, B. C.; Mujsce, A. M. *J. Am. Chem. Soc.* **2001**, *123*, 9214−9215.
(21) Laquindanum, J. G.; Katz, H. E.; Lovinger, A. J.; Dodabalapur, A. *Chem. Mater.* **1996**, *8*, 2542−2544.
(22) Hill, I. G.; Mäkinen, A. J.; Kafafi, Z. H. *J. Appl. Phys.* **2000**, *88*, 889−895.
(23) Watkins, N. J.; Zorba, S.; Gao, Y. *J. Appl. Phys.* **2004**, *96*, 425−429.
(24) Watkins, N. J.; Yan, L.; Gao, Y. *Appl. Phys. Lett.* **2002**, *80*, 4384−4386.

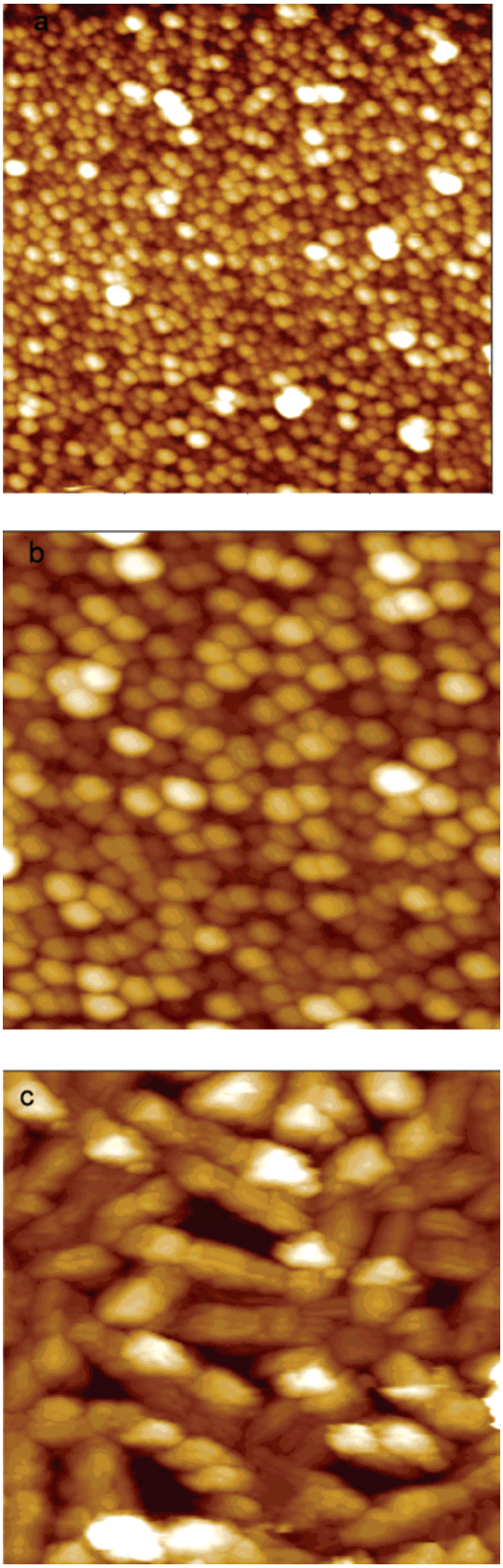

Figure 5. (a) A $5 \times 5\ \mu m^2$ AFM image of PTA film on SiO_2/Si fabricated at T_{sub} = room temperature. (b) A $5 \times 5\ \mu m^2$ AFM image of PTA film on SiO_2/Si fabricated at T_{sub} = 60 °C. (c) A $5 \times 5\ \mu m^2$ AFM image of PTA film on SiO_2/Si fabricated at T_{sub} = 80 °C. All of the AFM images were taken in contact mode.

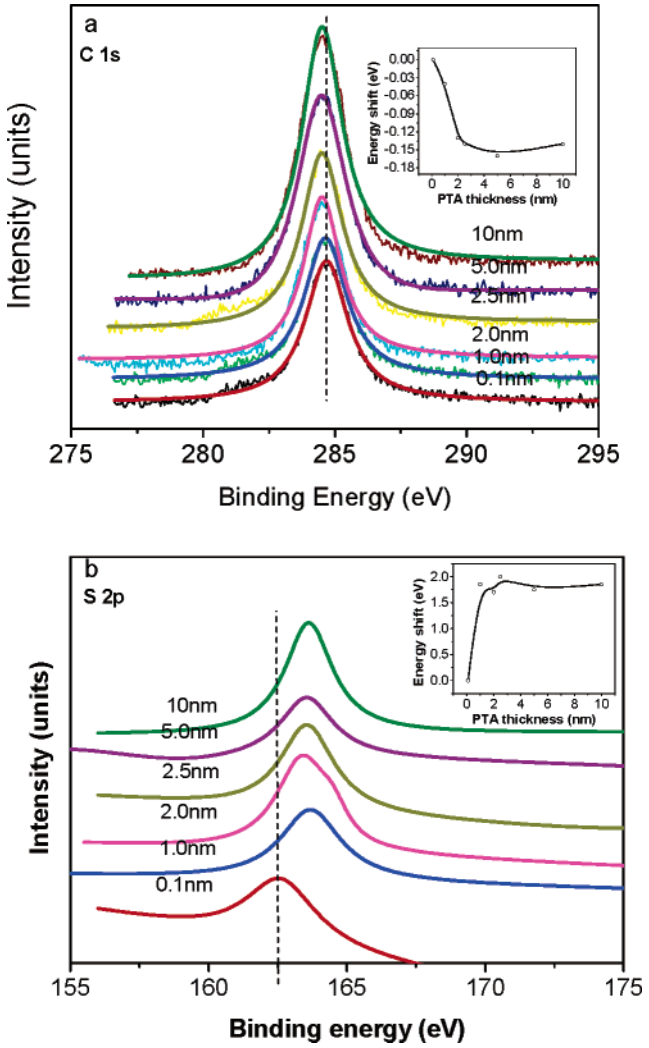

Figure 6. (a) XPS C 1s peaks of PTA deposition onto Au substrate. Inset shows binding energy shifts at the interface PTA/Au. (b) The XPS S 2p peaks of PTA deposition onto Au substrate. Inset shows binding energy shifts at the interface PTA/Au.

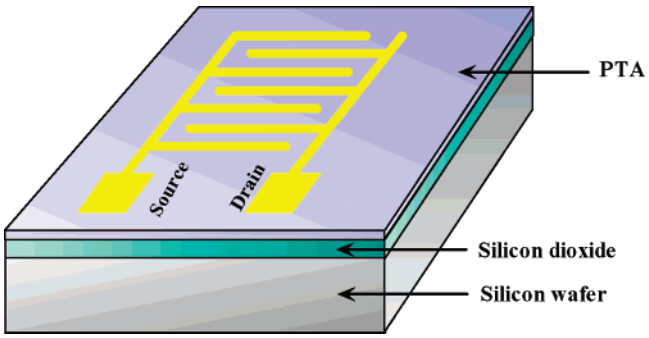

Figure 7. The device structure of the OTFT.

On the basis of ultraviolet photoelectron spectra (UPS) of PTA film prepared by vacuum deposition, Sato et al. have disclosed a strong intermolecular interaction, a kind of electron exchange due to intermolecular orbital interactions in solid film PTA. They also assumed that a kind of self-assembling interaction is operative in the hydrogen-poor, lengthy PTA π molecules.[13b]

OFETs of PTA were constructed on SiO_2/Si substrates by high-vacuum evaporation at different substrate temperatures using top-contact geometry (Figure 7).

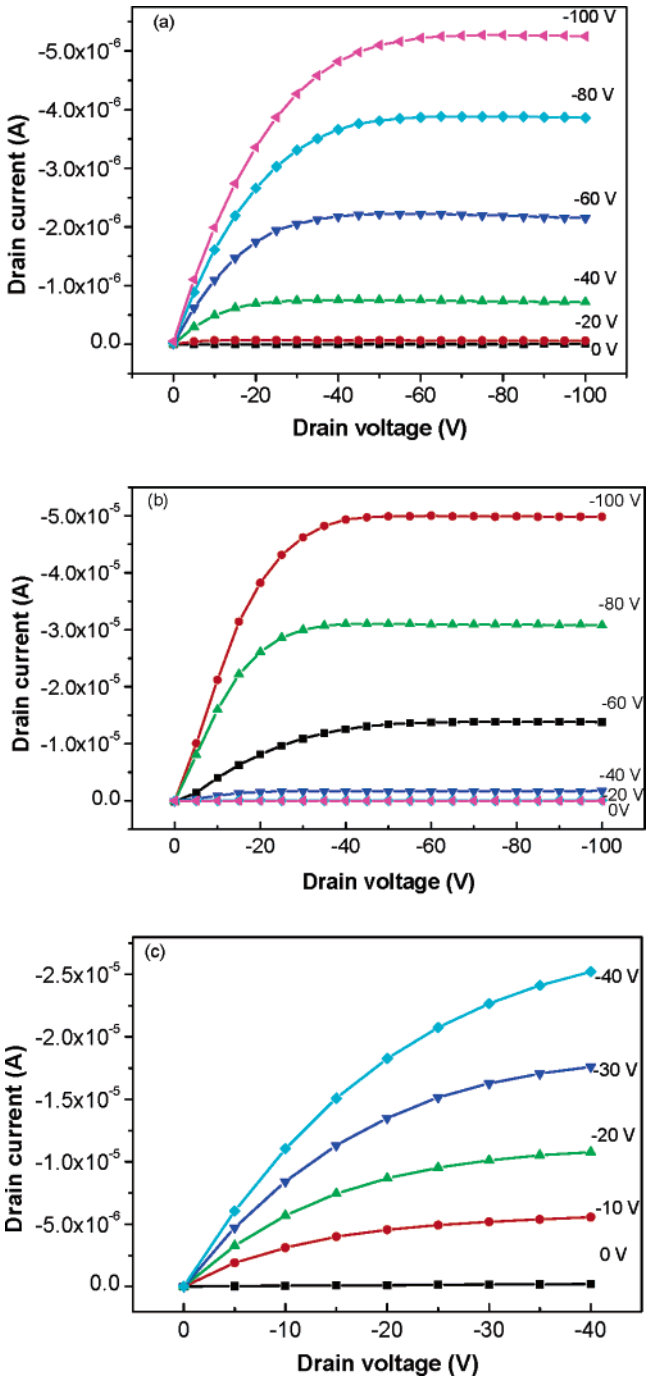

Figure 8. Drain current versus drain voltage as a function of gate voltage for OFETs with PTA at different substrate temperatures. (a) T_{sub} = room temperature; (b) T_{sub} = 60 °C; (c) T_{sub} = 80 °C.

The electrical measurements were performed at room temperature in the air. Figure 8 shows the drain current (I_d) versus drain voltage (V_d) characteristics for OFET with PTA at various gate voltages (V_g), which show very good saturation behaviors with clear saturation currents. The PTA displayed p-type accumulation FET behavior when used as channel semiconductor in OTFTs. The hole mobilities were calculated in the saturation regime, and the results for PTA obtained at different T_{sub} are summarized in Table 1. There is an energy barrier (0.23 eV) between the Au source/drain (S/D) electrodes and the HOMO of PTA (HOMO = 5.33 eV). Unlike the case in organic light-emission diodes, this does not present a serious problem, because the FET channel becomes highly conducting in the on state due to the large induced charge density.[25] Thus, the energy barrier between the Au contacts and the PTA HOMO is unlikely to be the cause of the change of sub-square-law behavior. The FET performances were dramatically improved with the deposition conditions and device geometry. It has been previously reported that the mobility of most organic semiconductors strongly depends on the T_{sub}.[26] In general, the mobility increases with increasing T_{sub}, which is attributed to better ordered thin films and larger grain sizes at elevated T_{sub}. Indeed, X-ray diffraction patterns showed higher diffraction intensity for thin films of the same thickness deposited at higher T_{sub}. The atomic force micrographs also showed sharper grain boundaries and larger crystal sizes for higher T_{sub} thin film. For example, the grain sizes for PTA were on the order of 300−600 nm at T_{sub} = 30 °C. The grain sizes became much bigger at elevated T_{sub} = 80 °C, on the order of 2−3 μm. The best mobility thus far achieved is 0.045 cm^2/V s with PTA at a substrate temperature of 80 °C. These mobilities are still lower than that of pentacene, but this value may be further improved by careful purification of the semiconducting materials and surface modification of the dielectric and contact electrode.

Table 1. Mobilities of PTA OFETs Prepared at Different Substrate Temperatures (T_{sub}) Using the Top-Contact Geometry

T_{sub} (°C)	mobility (cm^2/V s)	on/off ratio	grain sizes (μm^2)
rt	0.0043	10^3-10^5	0.3 × 0.6
60	0.011	10^2-10^5	0.8 × 1.0
80	0.045	10^2-10^3	0.8 × 2.5
100	no field effect	−	−

Conclusion

In summary, we have demonstrated that linearly condensed fused-ring pentathienoacene represents a new class of p-channel semiconductor with good stability owing to their large band gap. The fused-ring thiophene showed high mobility of 0.045 cm^2/V s. This stable organic semiconductor similar to pentacene would be extremely valuable for the application in organic electronics.

Acknowledgment. The authors gratefully acknowledge financial support from the National Natural Science Foundation of China (90206049, 20472089), the Major State Basic Research Development Program, and the Chinese Academy of Sciences.

Supporting Information Available: Instrumentation, materials synthesis and characterization, and OTFT fabrication. This material is available free of charge via the Internet at http://pubs.acs.org.

JA052816B

(25) (a) Ostrick, J. R.; Dodabalapur, A.; Torsi, L.; Lovinger, A. J.; Kwock, E. W.; Miller, T. M.; Galvin, M.; Berggren, M.; Katz, H. E. *J. Appl. Phys.* **1997**, *81*, 6804−6808. (b) Chua, L.; Zaumseil, J.; Chang, J.; C.-W. Ou, E.; K.-H. Ho, P.; Sirringhaus, H.; Friend, R. H. *Nature* **2005**, *434*, 194−199.

(26) Bao, Z.; Lovinger, A. J.; Dodabalapur, A. *Adv. Mater.* **1997**, *9*, 42−44.